Contribution from the School of Chemical Sciences,
University of Illinois, Urbana, Illinois 61801

Synthesis and Physical Properties of *meso*-Tetraferrocenylporphyrin, the Copper Complex, and the Corresponding Mixed-Valence Oxidation Products

RONALD G. WOLLMANN and DAVID N. HENDRICKSON*[1]

Received April 26, 1977 AIC70295E

The synthesis of *meso*-tetraferrocenylporphyrin, H_2TFcP, is reported. Many chemical and physical properties of black H_2TFcP are similar to those of other meso-substituted porphyrins. Metalation of H_2TFcP with Cu(II) gives tetraferrocenylporphyrincopper(II), Cu(TFcP). The compound H_2TFcP is characterized with infrared (porphyrin and ferrocene bands) and ^{57}Fe Mössbauer (ferrocene signal) spectroscopies. The ^1H NMR spectra (60, 100, and 220 MHz) indicate the presence of atropisomers which could not be separated by chromatographic techniques. The presence of the atropisomers leads to broad bands in the electronic absorption spectrum of H_2TFcP with a resolved absorption at 350 nm (ϵ 1.9×10^4 M^{-1} cm^{-1}) and a partially resolved absorption at 450 nm (ϵ 1.3×10^4 M^{-1} cm^{-1}). Structural models show that the dihedral angle between the planes of the porphyrin and the unsubstituted cyclopentadienyl rings of the four ferrocenes is small (ca. 15°); the shifting of the Soret band from the normal 400 nm position to 350 nm is explained by a π-electron interaction between the porphyrin and the ferrocenyl groups. Oxidation with either I_2 or DDQ (2,3-dichloro-5,6-dicyano-1,4-benzoquinone) of H_2TFcP gives $[H_2TFcP](I_3)_3$ or $[H_2TFcP](DDQH)_3$, and oxidation of Cu(TFcP) with I_2 gives $[Cu(TFcP)](I_3)_2$. Variable-temperature (4.2–270 K) magnetic susceptibility shows that all three compounds possess three unpaired electrons and that there are no magnetic exchange interactions present. EPR spectra for the three oxidized compounds indicate that these mixed-valence compounds are localized on the EPR time scale. The 295 K ^{57}Fe Mössbauer spectra for the three compounds also indicate localized systems; i.e., the thermal electron-transfer rates at room temperature between ferrocene and ferricenium centers are less than ca. 10^7 s^{-1}. Upon lowering the temperature of the three oxidized compounds to 90 K, the Mössbauer spectra show that the ferrocene-to-ferricenium ratio increases as indicated by fitting the areas of the two doublets. A migration of unpaired electron density from the ferricenium centers to the porphyrin ring at low temperatures is proposed to explain the observed temperature dependence of the ^{57}Fe Mössbauer spectra.

Introduction

During the past decade, interest in the porphyrin and metalloporphyrin field has increased. The importance and volume of work in this area have been emphasized by the recent appearance of an ambitious and thorough review.[2] Metalloporphyrins are indigenous to many biologically active molecules, particularly to several electron-transfer proteins found in electron transport chains.[3,4] The most thoroughly studied electron-transfer protein is cytochrome *c*. An electron is shuttled into and out of the iron porphyrin site as cytochrome *c* functions in the electron transport chain. Several mechanisms of electron transfer have been proposed.[5] Two mechanisms are of contemporary interest. In one mechanism, the coplanar alignment of the two tyrosine phenyl groups which line the "left" and "right" channels provide the pathway for electron transfer to and from the iron ion.[6-8] The electron transfers by "hopping" along the aligned phenyl groups. In the second mechanism, the electron transfer is effected by an outer-sphere interaction of an electron-donor or -acceptor molecule with the exposed edge of the iron porphyrin unit.[9,10]

Mixed-valence compounds provide a means of studying thermal electron transfer.[11,12] Recent work on mixed-valence biferrocenes indicates that the thermal transfer of an electron from the Fe(II) ion to the Fe(III) ion is probably propagated through the electron density of the cyclopentadienyl rings and the bridging moiety.[13-15] The ferrocene–ferricenium couple can, thus, provide a gauge of the viability of a particular bridging molecular fragment for thermal electron transfer. This led us to prepare for the first time *meso*-tetraferrocenylporphyrin (H_2TFcP). In this paper, we report the synthesis and characterization of H_2TFcP, the Cu(II) derivative, Cu(TFcP), and several mixed-valence compounds that are derived from these two compounds.

Experimental Section

Compound Preparations. Samples of *meso*-tetraferrocenylporphyrin, H_2TFcP, were prepared by a procedure similar to that used to prepare *meso*-tetraphenylporphyrin.[16] Four grams of formylferrocene (purchased from Alfa Products) was dissolved in refluxing propanoic acid (ca. 20 mL). With stirring, pyrrole (ca. 1 mL) was added dropwise. The solution was stirred for 30 min, cooled rapidly, and filtered. The resulting black powder was washed thoroughly with methanol until the washings were colorless. After drying, the black solid was dissolved in a minimal amount of $CHCl_3$ (ca. 50 mL) and chromatographed on an alumina column (Alcoa Chemicals, F-1 48–100 activated alumina). Elution with $CHCl_3$ resulted in the separation of three bands. The first band was yellow-greenish black, the second was reddish black (very small quantity of compound), and the third was black. The first two bands were removed rapidly from the column with $CHCl_3$. The third band, which was adsorbed strongly, was removed from the column by elution with Me_2SO. A small amount of $CHCl_3$ (ca. 50 mL) was added to the Me_2SO solution of band three and the resulting solution was washed five times with an equal volume of water. The organic layer was then evaporated to dryness and dried in vacuo over P_4O_{10} to give $H_2TFcP \cdot Me_2SO$ (2.1 g, 40% yield based on formylferrocene). Anal. Calcd for $C_{62}H_{52}N_4Fe_4SO$: C, 66.21; H, 4.67; N, 4.98; Fe, 19.86; S, 2.85; mol wt, 1124.64. Found: C, 66.17; H, 4.62; N, 5.28; Fe, 19.81; S, 1.55; effective mol wt in $CHCl_3$, 759 as determined by vapor pressure osmometry.

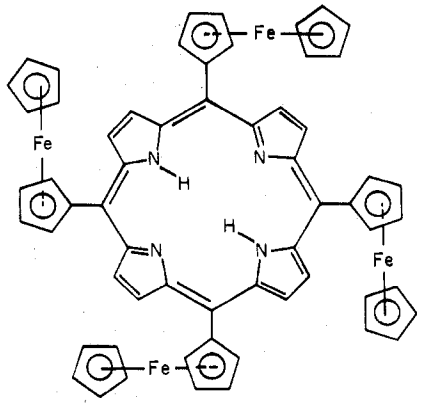

H_2TFcP

Recrystallization of $H_2TFcP \cdot Me_2SO$ from $CHCl_3$ four times resulted in the isolation of black microcrystals. These microcrystals were washed with H_2O and dried in vacuo over P_4O_{10} to yield $H_2TFcP \cdot 2CHCl_3$. Anal. Calcd for $C_{62}H_{48}N_4Fe_4Cl_6$: C, 57.94; H, 3.77; N, 4.36; Fe, 17.38; Cl, 16.55; mol wt, 1285.24. Found: C, 57.46;

H, 3.79; N, 4.23; Fe, 17.25; Cl, 12.57; effective mol wt in $CHCl_3$, 2037.

Tetraferrocenylporphyrincopper(II), Cu(TFcP), was synthesized by a general procedure described previously for the preparation of metalloporphyrins.[17] Copper acetate (ca. 0.5 g) was dissolved in refluxing DMF (ca. 60 mL), and then, with stirring, a DMF solution (ca. 60 mL) of $H_2TFcP \cdot Me_2SO$ (ca. 0.5 g) was added. The solution was stirred at reflux temperature for 5 min, cooled rapidly, and filtered. An equal volume of H_2O was added to the rapidly stirred DMF filtrate in order to cause precipitation. The precipitate was extracted with $CHCl_3$. The $CHCl_3$ solution was washed with H_2O and then evaporated to dryness. The resulting solid was washed with diethyl ether and dried to obtain the black powder Cu(TFcP)·2DMF Anal. Calcd for $C_{66}H_{58}N_6Fe_4CuO_2$: C, 63.20; H, 4.67; N, 6.70; Fe, 17.80; Cu, 5.07. Found: C, 62.22; H, 4.18; N, 5.32; Fe, 17.52; Cu, 4.92.

Recrystallization of Cu(TFcP)·2DMF from $CHCl_3$ resulted in the isolation of black microcrystalline needles. The crystals were washed with H_2O and dried in vacuo over P_4O_{10} to yield Cu(TFcP)·DMF·2$CHCl_3$. Anal. Calcd for $C_{65}H_{53}N_5Fe_4CuCl_6O$: C, 54.98; H, 3.77; N, 4.93; Fe, 15.73; Cu, 4.48. Found: C, 55.59; H, 3.70; N, 4.80; Fe, 15.65; Cu, 4.49.

$[H_2TFcP](I_3)_3$. The compound $H_2TFcP \cdot Me_2SO$ (100 mg) was dissolved in $CHCl_3$ (ca. 5 mL) and filtered. A $CHCl_3$ solution (ca. 15 mL) of iodine (150 mg) was added dropwise with rapid stirring to the $H_2TFcP \cdot Me_2SO$ solution. A black precipitate formed immediately and the resulting suspension was stirred for 15 min and then filtered. The resulting black powder was washed with diethyl ether (ca. 30 mL) and then dried on a vacuum line for 12 h. Anal. Calcd for $C_{60}H_{46}N_4Fe_4I_9$: C, 32.91; H, 2.12; N, 2.56; Fe, 10.21; I, 52.18. Found: C, 31.62; H, 2.19; N, 2.32; Fe, 9.94; I, 52.43.

$[H_2TFcP](DDQH)_3$. The compound $H_2TFcP \cdot Me_2SO$ (100 mg) was dissolved in $CHCl_3$ (ca. 5 mL) and filtered. A benzene solution (ca. 10 mL) containing 100 mg of 2,3-dichloro-5,6-dicyano-1,4-benzoquinone (DDQ) was added dropwise with rapid stirring. A black precipitate formed immediately and the resulting suspension was stirred for several minutes and then filtered. The resulting black solid was washed with diethyl ether until the washings were colorless. The black solid was dried in vacuo over P_4O_{10}. Anal. Calcd for $C_{84}H_{49}N_{10}Fe_4Cl_6O_6$: C, 58.30; H, 2.86; N, 8.10; Fe, 12.91. Found: C, 57.14; H, 2.92; N, 7.41; Fe, 12.91.

$[Cu(TFcP)](I_3)_2$. A sample of Cu(TFcP)·2DMF (100 mg) was dissolved in $CHCl_3$ (ca. 15 mL) and filtered. Iodine (150 mg) was dissolved in $CHCl_3$ (ca. 15 mL) and this solution was added dropwise with rapid stirring to the Cu(TFcP) solution. A fine black precipitate formed immediately and the suspension was stirred for 30 min. The suspension was cooled to 5 °C and filtered. The resulting black solid was washed with diethyl ether (ca. 30 mL) and dried on a vacuum line for 14 h. Anal. Calcd for $C_{60}H_{44}N_4Fe_4CuI_6$: C, 38.55; H, 2.38; N, 3.00; Fe, 11.95; Cu, 3.40. Found: C, 37.48; H, 2.52; N, 3.07; Fe, 11.06; Cu, 3.08.

Physical Measurements. Infrared spectra were obtained with a Perkin-Elmer Model 467 spectrophotometer. Samples were prepared as 13-mm KBr pellets. A Cryogenics Technology, Inc. "Spectrim" closed-cycle helium gas refrigerator, equipped with 50 × 4 mm KBr windows, was used to obtain low-temperature IR spectra. The lowest sample temperature obtainable is between 20 and 30 K, as described previously.[18]

Variable-temperature (4.2–270 K) magnetic susceptibility data were obtained with a PAR Model 150A vibrating-sample magnetometer. Temperatures were monitored with a Lake Shore Cryotronics, Inc., Model TG-100 P/M temperature-sensitive GaAs diode. The GaAs diode was calibrated by obtaining a complete (4.2–270 K) susceptibility curve for $CuSO_4 \cdot 5H_2O$.

Varian E-line EPR spectrometers were used to obtain EPR spectra. The details of equipment and sample temperatures are found in a previous paper.[12]

Iron-57 Mössbauer spectra were obtained at 4.2 K with an instrument that has been previously described.[19] Room-temperature and 90 K spectra were obtained with a second instrument.[20] Computer fittings of the Mössbauer data to Lorenztian curves were performed with a modified version of a previously reported program.[21]

Electronic absorption spectra were run with a Cary Model 14 spectrophotometer. Solution spectra were obtained with quartz cells of 1-cm path length. Room-temperature and 77 K solid-state absorption spectra were obtained for 13-mm pressed disks consisting of 0.1 mg of sample and 100 mg of KBr. A 13-mm KBr disk (100 mg) was used in the reference beam. For low-temperature measurements, a quartz Dewar was employed.

Varian Models A60, HA100, and HR220 spectrometers were used to obtain ^1H NMR spectra. Low-temperature ^1H spectra at −60 °C were obtained using the HA100 and HR220 spectrometers. A Jeol Ltd. Model FX60 spectrometer was used to obtain ^{13}C NMR spectra. All ^{13}C spectra were proton and noise decoupled and Me_4Si was used as an internal reference.

Results and Discussion

Tetraferrocenylporphyrin, H_2TFcP. Simplified methods for the synthesis[16] and purification[22,23] of meso-substituted porphyrins have been developed. Such synthetic procedures are well suited for condensing aromatic aldehydes with pyrroles.[16,24] Consequently, we felt that formylferrocene should readily condense with pyrrole in refluxing propanoic acid to form a new meso-substituted porphyrin, *meso*-tetraferrocenylporphyrin.

A black solid precipitates from the reaction of formylferrocene with pyrrole in propanoic acid. The solid is very soluble in Me_2SO, DMF, and $CHCl_3$, somewhat soluble in other solvents such as benzene and xylene, and insoluble in alcohols, ethers, and water. Purification of H_2TFcP by column chromatography on alumina results in the separation of three bands when eluted with $CHCl_3$. The first two bands are, respectively, yellow-black and red-black and the third is black. By far, the majority of the compound is contained in the third band and in the following it will be shown that this black compound is H_2TFcP. It is possible that the first and second bands are the corresponding chlorin and phlorin.

The mechanism of formation of porphyrins by the polymerization of monopyrroles has been investigated by Adler.[25] Condensation of one pyrrole with an aldehyde molecule to form a pyrrylcarbinol is postulated as the initial step of the reaction. Further condensation leads to the formation of di-, tri-, tetra-, and poly(pyrryl)methane- and -methenecarbinols as intermediates. Ring closure of the tetrapyrrylcarbinols results in the formation of porphrinogens, chlorins, phlorins, dihydrochlorins, dihydrophlorins, and porphyrins. Further oxidation of the resulting saturated ring structures by oxygen leads to the isolation of minor amounts of chlorine and phlorins and major amounts of porphyrins.

The possibility that the third band in the H_2TFcP synthesis is an open-chain tetrapyrrylmethane can be discounted, because isolated tetrapyrrylmethanes are almost colorless solids.[26] Porphrinogens are also known to be colorless as a result of the disruption of the ring conjugation,[27] and, as such, the black compound in band three is *not* a porphrinogen. Thus, the third band possesses the characteristics of a porphyrin and not those of open-chain condensation products.

Because a ferrocenyl unit is relatively large, steric interactions are expected to exist between the ferrocenyl groups and the porphyrin ring. Relative to the plane of the porphyrin ring, the two orientations of a ferrocenyl group which result in maximum steric interactions occur when the dihedral angle between the plane of the porphyrin ring and the plane of the substituted cyclopentadienyl ring is either 0 or 90°. Representative bond lengths and angles from previous x-ray crystallographic data for free-base porphyrins[28,29] and ferrocenes[30,31] have been used to construct the diagrams in Figure 1 to illustrate these two conformations. Planarity of the porphyrin ring and rigidity of the ring–metal–ring axes of the ferrocenyl unit have been assumed. In the 0° case, there is a ca. 1.0 Å separation between the hydrogen atoms of the C_β atoms and the hydrogen atoms of C_2 and C_5 on the ferrocenes. The corresponding distance for H_2TPP is ca. 0.8 Å. The nonbonded pair potential energy has been calculated to be quite large for H_2TPP with the 0° dihedral angle.[32] The steric interactions would be expected to be less for H_2TFcP in the 0° conformation. However, the pair potential energies would

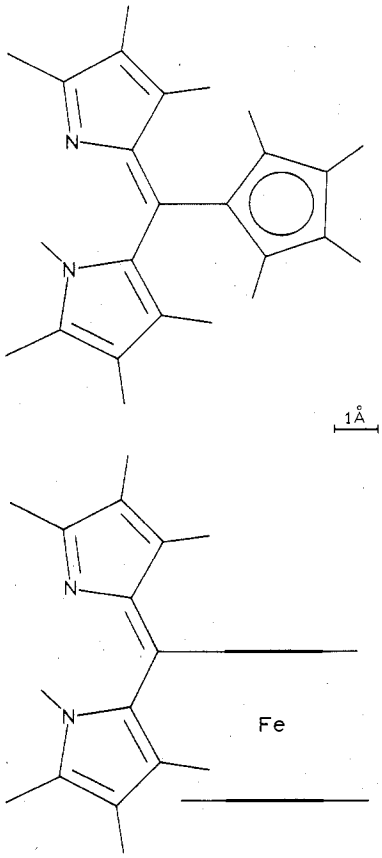

Figure 1. Structural diagrams for a fragment of H_2TFcP when the dihedral angle between the plane of the porphyrin and the plane of the substituted cyclopentadienyl ring is 0° (top) and 90° (bottom).

still be expected to be large enough in H_2TFcP to lead to an equilibrium orientation of the ferrocenyl groups that is somewhat removed from the 0° dihedral angle.

As illustrated in Figure 1, the 90° orientation for the ferrocenyl groups of H_2TFcP leads to quite large nonbonded potential energy terms. In this case, one of the hydrogen atoms of the pyrrole moiety contacts parts of the unsubstituted cyclopentadienyl ring and the iron atom. As a result of these steric interactions, an equilibrium orientation of the ferrocenyl groups substantially removed from the 90° dihedral angle would be expected. In reality, the ferrocene groups and porphyrin framework probably distort to allow, at best, a restricted rotation of the ferrocenyl groups in solution. In the solid state, the ferrocenyl groups probably have dihedral angles that deviate somewhat from 0°. A reasonable estimate for the equilibrium dihedral angle would be on the order of 15°.

The restricted rotation of the ferrocenyl groups of H_2TFcP in solution leads to the possible presence of four atropisomers as sketched in Figure 2. The statistical distribution of these four atropisomers is 1:4:2:1. Atropisomerism has been observed for several other meso-tetrasubstituted porphyrins.[33-35] In some cases the four atropisomers have been successfully separated by chromatography on silica. Attempts to separate the four atropisomers of H_2TFcP have been unsuccessful. Thin-layer chromatography on silica or alumina using either chloroform or 1:1 chloroform–diethyl ether does not indicate any separation.

Although the atropisomers of a meso-substituted porphyrin may not be physically separable, the rate of isomerization may be slow enough to allow the detection of the four atropisomers with NMR (rate less than ca. 10^6 s^{-1}). Such is the case for the metal complexes of *meso*-tetra-*o*-tolylporphyrin. For example, physical separation of the four atropisomers of the nickel complex of this porphyrin has not proven to be possible.

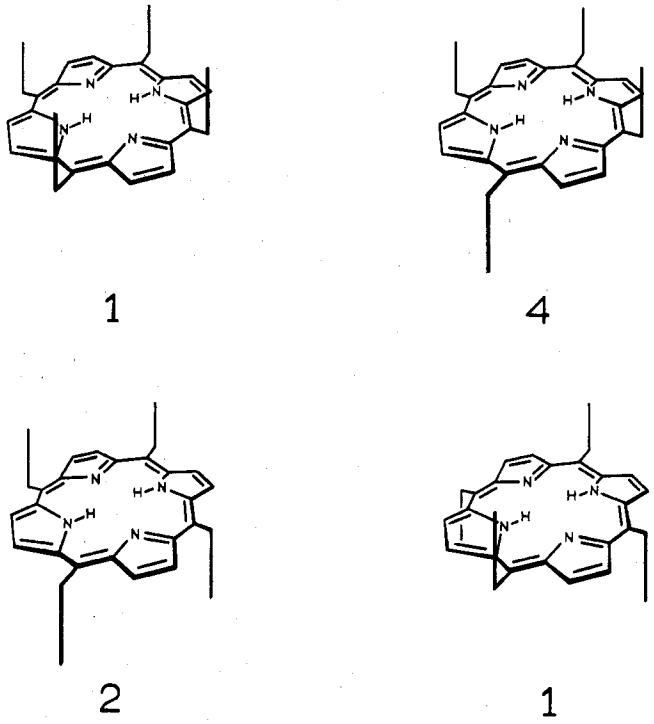

Figure 2. Schematic representation of the four atropisomers of H_2TFcP. The lines normal to the plane of the porphyrin represent the ring–metal–ring axes of the ferrocenyl groups. The relative statistical ratio is given below each atropisomer.

However, multiple methyl group resonances in the ^1H NMR spectrum do indicate the presence of four distinct atropisomers in the NMR spectrum.[34]

The ^1H NMR spectra of $H_2TFcP \cdot Me_2SO$ obtained at various frequencies (220, 100, and 60 MHz) and temperatures (213–300 K) do indicate the presence of atropisomers. In all cases, the spectra consist of a weak, broad resonance at 2.59 ppm downfield from Me_4Si, a strong, broad multiplet in the 4.0–5.0-ppm region, and several weak, broad resonances in the 6.0–8.0-ppm region. There is no temperature dependence in the spectrum except for broadening due to increased solvent viscosity at low temperatures. The 100- and 220-MHz ^1H NMR spectra of a room temperature $CDCl_3$ solution are shown in Figure 3. The multitude of resonances and broadness of peaks are reflections of the presence of atropisomers. The four atropisomers in the 1:4:2:1 statistical ratios correspond to the "4 up", "3 up, 1 down", "2 up, 2 down-cis", and "2 up, 2 down-trans" configurations. Each of the atropisomers, except one, has only one type of ferrocene (see Figure 2). The "3 up, 1 down" isomer has three inequivalent ferrocenyl groups in the relative ratios of 1:2:1. Thus, for the nonsubstituted cyclopentadienyl rings six different ^1H resonances would be expected with intensities of 1:1:2:1:2:1 (if the distributions are statistical). Each of the six inequivalent substituted rings has two pairs of inequivalent hydrogens which may result in two triplet resonances. Consequently, up to 36 possible resonances may originate from the six inequivalent substituted cyclopentadienyl rings. The six inequivalent ferrocenyl groups also give rise to six sets of inequivalent C_β hydrogens with their corresponding resonances.

Certain peaks can be assigned in the 220-MHz spectrum (Figure 3). The resonance at 2.59 ppm is due to Me_2SO and the sharp peak at 7.25 ppm results from the $CHCl_3$ impurity in the $CDCl_3$ solvent. The broad resonances at 5.80, 6.10, 6.62, 7.52, and 7.98 can be assigned to the C_β hydrogen atoms. Chemical shifts of 9.74 and 8.75 ppm have been observed for the C_β hydrogens of porphine[36] and H_2TPP,[37] respectively. The higher field chemical shift observed for H_2TPP as compared

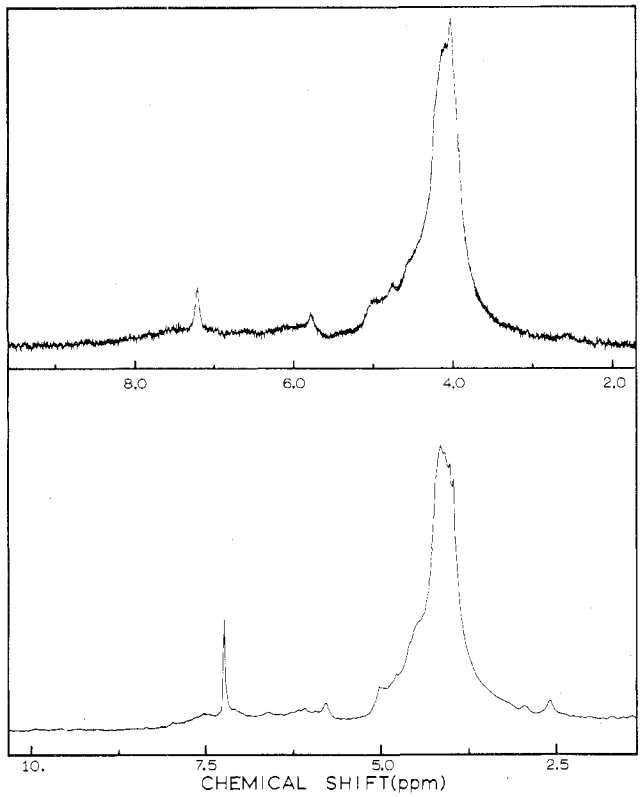

Figure 3. Room temperature ^1H NMR spectra of a $CDCl_3$ solution of $H_2TFcP\cdot Me_2SO$ at 100 MHz (top) and 220 MHz (bottom). Chemical shifts are referenced to internal Me_4Si standards.

to porphine results from the shielding effect of the phenyl groups. Ferrocenyl substituents would be expected to have an even more pronounced shielding effect as a neighboring group to the C_β hydrogen atoms.

The broad multiplet in the 4.0–5.0 ppm region is assigned to the various hydrogen atoms of the ferrocenyl groups. As can be seen in Figure 3, resolved or partially resolved resonances can be seen at 3.98, 4.03, 4.10, 4.16, 4.24, 4.26, 4.45, 4.59, 4.79, and 5.03 ppm in the room temperature 220-MHz spectrum. For comparison, resonances assigned to the hydrogens of C_6, $C_{3,4}$, and $C_{2,5}$ for phenylferrocene have chemical shifts of 3.87, 4.14, and 4.47 ppm, respectively.[38]

Atropisomerism may also be observed with ^{13}C NMR. However, the resonances of atropisomers are usually not as well resolved in ^{13}C NMR spectra as compared to ^1H spectra.[39,40] This is understandable in the sense that proton chemical shifts can be affected markedly by neighboring group effects, whereas carbon chemical shifts are largely determined by electronic effects in the immediate vicinity. The room temperature ^{13}C NMR spectrum of $H_2TFcP\cdot Me_2SO$ in $CDCl_3$ is shown in Figure 4. A ^{13}C spectrum was also run in Me_2SO-d_6 solution. In the case of the $CDCl_3$ spectrum in Figure 4, the strong resonances at 79.2, 77.1, and 75.0 ppm downfield from Me_4Si are attributable to $CDCl_3$. Also, there is a resonance at 38.2 ppm (not shown in Figure 4) for the Me_2SO in the sample.

In previous ^{13}C NMR investigations on several meso-substituted porphyrins, the C_α, C_β, and C_m resonances have been assigned to peaks in the 90–151-ppm region.[39,40] The C_α resonance has been found to have the largest chemical shift followed by the C_β resonance with the C_m resonance having the smallest chemical shift of the three. Broadening due to N–H tautomerism has been used to assign the C_α resonances, and broadening from deuteration of C_β has been used to assign the C_β resonances.

Three resonances are observed in the 90–151-ppm region

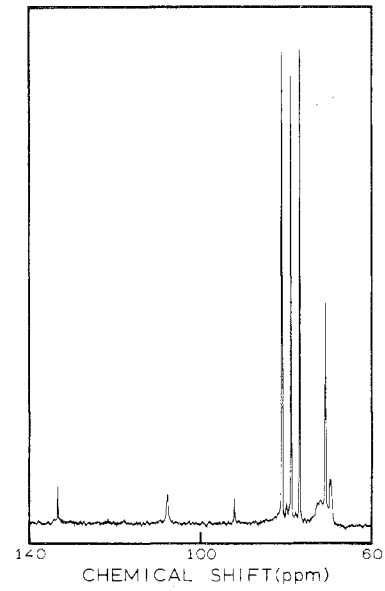

Figure 4. Room temperature ^{13}C NMR spectrum of $H_2TFcP\cdot Me_2SO$ dissolved in $CDCl_3$. Chemical shifts are referenced to an internal Me_4Si standard.

of the $H_2TFcP\cdot MeSO$ spectrum. The resonance at 90.4 ppm is probably due to C_m. Tentatively, the resonances at 132.2 and 106.3 ppm can be assigned to C_β and C_α, respectively. Broadness of the 106.3-ppm peak may be the result of N–H tautomerism and the greater intensity of the 132.2 ppm resonance may be attributed to the nuclear Overhauser effect which should enhance the C_β resonance relative to the C_α and C_m resonances. These assignments of the C_α and C_β resonances are reversed from the previous assignments.[39,40] which could reflect the effect of the presence of the ferrocenyl groups.

The remainder of the peaks in the $H_2TFcP\cdot Me_2SO$ ^{13}C spectrum are assignable to the carbon atoms of the ferrocenyl groups. Carbon-13 NMR data have been reported for several monosubstituted ferrocenes.[41] Chemical shifts in the range of 69.3–70.3 ppm downfield from the Me_4Si have been observed for the C_6 carbon atoms of the unsubstituted rings. The chemical shifts for the $C_{2,5}$ and $C_{3,4}$ carbons have been observed in the ranges of 67.1–70.8 and 70.6–72.9 ppm, respectively, and for the C_1 carbon atoms in the relatively large range of 77.8–85.6 ppm. For monosubstituted ferrocenes, *chemical shift ranges* increase in the order of $C_6 < C_{3,4} < C_{2,5} < C_1$. In addition, the *chemical shifts* for a particular monosubstituted ferrocene are usually in the order of $C_{2,5} < C_6 < C_{3,4} < C_1$.

The ferrocene region of the ^{13}C NMR spectrum of $H_2TFcP\cdot Me_2SO$ shows several peaks. Because the C_6 carbons of the unsubstituted rings show a small range of shifts, it is doubtful that the C_6 carbons of the *six* possible inequivalent ferrocenyl groups of the four atropisomers would be resolved. The strong resonance at 68.9 ppm is, thus, probably associated with all of the various C_6 carbon atoms. The resonances at 67.6 and 67.9 ppm may be assigned to the $C_{2,5}$ atoms, while the broader resonances at 70.2 and 70.8 ppm may be assigned to the $C_{3,4}$ atoms. There are two resonances at 76.1 and 78.3 ppm among the strong $CDCl_3$ resonances and these could be some of the expected C_1 resonances. Attempts to better observe C_1 resonances for the six inequivalent ferrocenyl groups by obtaining a room temperature ^{13}C spectrum of $H_2TFcP\cdot Me_2SO$ in Me_2SO were *not* successful due to a decreased solubility and resultant reduced signal-to-noise ratio.

A single quadrupole–split doublet is observed in the ^{57}Fe Mössbauer spectrum of $H_2TFcP\cdot Me_2SO$ at 100 K. The spectrum is devoid of signs of other signals. The one doublet can be least-squares fit to give a quadrupole splitting (ΔE_Q)

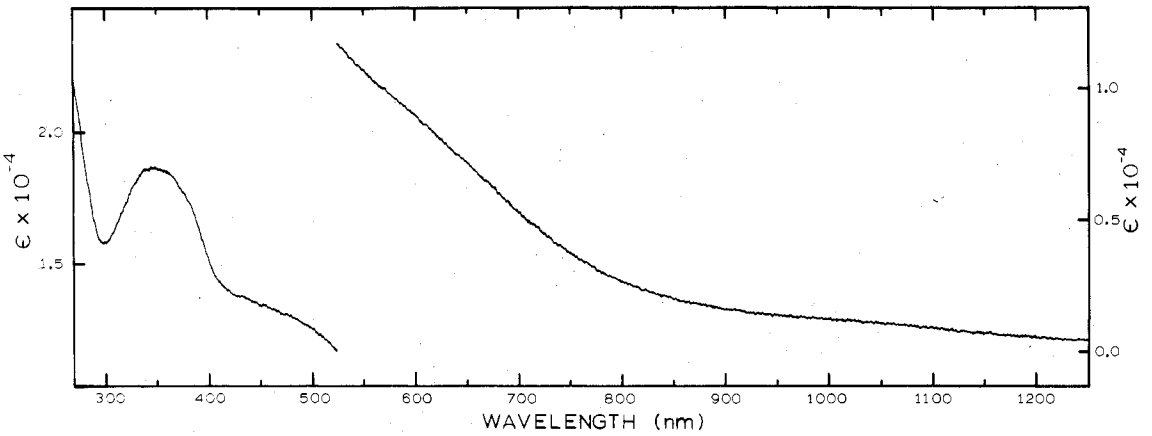

Figure 5. Room temperature electronic absorption spectrum of a $CHCl_3$ solution of $H_2TFcP \cdot 2CHCl_3$. The molar extinction coefficient (ϵ) is given in units of M^{-1} cm^{-1}.

at 100 K of 2.270 (6) mm/s and an isomer shift (δ) relative to iron metal of 0.415 (6) mm/s. These values are very similar to the values reported[42,43] for ferrocene: ΔE_Q = 2.38 mm/s and δ = 0.44 mm/s relative to iron metal. The line width for each component of the $H_2TFcP \cdot Me_2SO$ doublet at 100 K is 0.186 mm/s and this is reasonable for natural line widths. Thus, no difference in the Mössbauer parameters is indicated for the four atropisomers, as is expected.

Infrared spectra for $H_2TFcP \cdot Me_2SO$ and $H_2TFcP \cdot 2CHCl_3$ pelleted in KBr are similar to the spectra observed for other porphyrins. Peaks centered at 750, 1000, 1200, and 1400 cm^{-1} which are assigned to porphyrin skeleton vibrations have been observed for several meso-substituted porphyrins.[44] These groups of vibrations are also observed for the two H_2TFcP compounds. However, all of the absorptions in the spectra are broad, especially those at higher energies. Lowering the temperature of the KBr pellets to ca. 30 K does not affect the resolution. In addition to the porphyrin bands, there are two bands readily visible at 505 and 1110 cm^{-1} and these are characteristic of ferrocene.[45,46]

The room temperature electronic absorption spectrum of a $CHCl_3$ solution of $H_2TFcP \cdot 2CHCl_3$ is very diffuse with optical density extending out to ca. 1200 nm. A resolved absorption at 350 nm with a molar extinction coefficient (ϵ) of 1.9×10^{-4} M^{-1} cm^{-1} and a partially resolved absorption at 450 nm with ϵ 1.3×10^{-4} M^{-1} cm^{-1} are observed. This spectrum is shown in Figure 5. Samples of this same compound prepared as KBr pellets and maintained at 300 and 77 K gave very similar spectra with no improvement in resolution.

Generally, five bands in the 450–700-nm region and a very intense Soret absorption at ca. 400 nm are observed in the electronic absorption spectra of meso-substituted porphyrins.[24,47] The relative intensities and energies of the five visible bands are sensitive to the particular type of meso substituent. A comparison of the crystal structure data of porphine, H_2TPP, and tetra-*n*-propylporphyrin (H_2TPrP) suggests that the differences in intensities and energies result from localized changes of π-electron density in the porphyrin ring that is caused by small changes of bond lengths and angles involving the C_m carbon atoms.[48]

On the other hand, the Soret band is most affected by steric interactions resulting from substitutions at the C_β atoms. This is evidenced by a decrease of intensity by a factor of 4, a dramatic broadening, and a shift to slightly lower energy of the Soret absorption of octamethyltetraphenylporphyrin (H_2OMTPP) as compared to the Soret absorption of H_2TPP.[27] A comparison of the crystal structure data for porphine,[48] octaethylporphyrin (H_2OEP),[49] and mesoporphyrin IX dimethyl ester (H_2MP IX DME)[50] suggests that these differences result from decreases of π-electron density at the C_β atoms which are caused by increased bond lengths in the pyrrole rings and by canting and tilting of the pyrrole rings such that the porphyrin ring is nonplanar.

Both of the above effects could be present in H_2TFcP. The overall broadness and poor resolution of the electronic absorption spectra of H_2TFcP probably are attributable to the presence of the four atropisomers. For all of the cases in which atropisomers of other porphyrins have been successfully separated, each of the atropisomers has been reported to have identical electronic absorption spectra.[33,35] This, however, would probably not be expected for H_2TFcP. The potentially large steric interactions in H_2TFcP could easily cause each atropisomer to have absorptions shifted by 5–10 nm, which would result in broad, poorly resolved spectral features for the mixture. The presence of atropisomers could explain the poor resolution of the spectra, but it does *not* explain why bands are observed at 350 and 450 nm, and not at ca. 400 nm which is expected for a Soret band. For this explanation we turn to some additional facts.

High-spin manganese(III) porphyrins are noted for having a *pair* of Soret-like absorptions that are centered about 400 nm.[51] The higher energy bands at 350–360 nm have been assigned as Soret $\pi \rightarrow \pi^*$ transitions. The lower energy bands in the region of 470–480 nm have been assigned as ligand-to-metal charge-transfer transitions which gain intensity by mixing with the Soret $\pi \rightarrow \pi^*$ transitions.[51,52] Thus, these anomalous manganese(III) porphyrin spectra result from having metal d orbitals and porphyrin π orbitals that are of like symmetry and comparable energies to interact.

A similar interaction between the porphyrin and ferrocenyl group molecular orbitals could give rise to a similar anomalous absorption spectrum for H_2TFcP. As mentioned in the beginning of this section, the equilibrium dihedral angle between the porphyrin plane and the substituted cyclopentadienyl ring plane is most probably quite small. Ferrocene does have charge-transfer transitions in the 400-nm region. Thus, the 350-nm band for H_2TFcP may be the shifted Soret band and the 450-nm band may largely be a ferrocene-localized charge-transfer band. No other tetraarylporphyrins are known to have dihedral angles that are less than the 60° angle of H_2TPP.[2] Even for tricarbonylchromium π complexes of H_2TPP, where steric interactions of the $Cr(CO)_3$ moieties with the porphyrin ring might be expected, the dihedral angles are found to be large, and typical porphyrin electronic absorption spectra are observed.[53] Likewise, no molecular orbital calculation has been performed for an aromatic meso-substituted porphyrin wherein there is the potential for a strong interaction of the two types of π-electron systems. However, phthalocyanine, which has benzene rings fused onto the pyrrole rings,

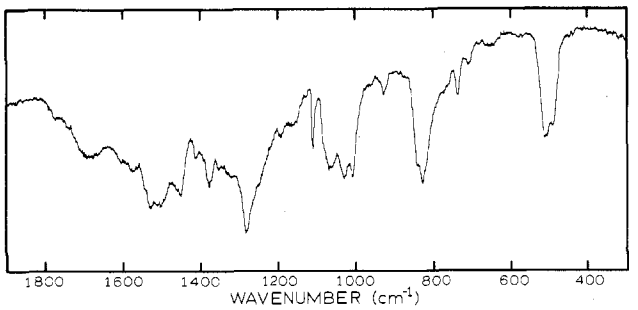

Figure 6. Room temperature, KBr-pellet infrared spectrum of $Cu(TFcP)\cdot DMF\cdot 2CHCl_3$.

provides a good example of what might be expected. Several intense Soret-like absorptions are observed in the electronic absorption spectrum of phthalocyanine.[54] Calculations indicate that several $\pi \rightarrow \pi^*$ and $n-\pi^*$ transitions may give rise to the observed bands.[55,56] Thus, it should not be surprising that the electronic absorption spectrum of H_2TFcP is different from those of other tetraarylporphyrins.

Tetraferrocenylporphyrincopper(II), Cu(TFcP). The free base H_2TFcP was metalated to give solvated Cu(TFcP). The success of this procedure and the properties of the resulting compound are further support for the fact that the compound H_2TFcP is a porphyrin.

The room temperature KBr pellet infrared spectrum of $Cu(TFcP)\cdot DMF\cdot 2CHCl_3$ is similar to that of the free base. There is, however, better resolution of the absorptions at energies greater than 1200 cm^{-1}. The spectrum is shown in Figure 6. As we indicated above, vibrations attributable to the porphyrin skeleton are centered at 800, 1000, 1300, and 1500 cm^{-1}. Characteristic ferrocene bands are observed at 505 and 1110 cm^{-1}. The broadness of the bands may again reflect the presence of four atropisomers. In all, the IR spectrum of $Cu(TFcP)\cdot DMF\cdot 2CHCl_3$ is typical of a metalloporphyrin.[44]

The room temperature electronic absorption spectrum of a $CHCl_3$ solution of $Cu(TFcP)\cdot DMF\cdot 2CHCl_3$, as illustrated in Figure 7, is also similar to the spectrum of $H_2TFcP\cdot 2CHCl_3$ in that it is diffuse and optical density extends out to about 1200 nm. A few additional features are resolved. Resolved peaks are observed at 360 and 507 nm with molar extinction coefficients of 2.5×10^4 and 1.9×10^4 M^{-1} cm^{-1}, respectively. Partially resolved peaks are seen at 424 and ca. 665 nm and these have uncorrected molar extinction coefficients of 1.9×10^4 and ca. 1.1×10^4 M^{-1} cm^{-1}, respectively. KBr pellet spectra at either 300 or 77 K do not show improved resolution. The comments that were made about the H_2TFcP spectrum are also applicable to the spectrum for the copper complex. The additional feature at 424 nm seems to be very minor, whereas the additional peak at ca. 665 nm could be the ligand field transition associated with the Cu(II) center.

Electron paramagnetic resonance data were obtained for $Cu(TFcP)\cdot 2DMF$ and compared to data for copper(II) porphyrins to give further substantiation for the presence of a porphyrin unit. An X-band EPR signal is not detected at 300 K for a solid sample of $Cu(TFcP)\cdot 2DMF$; however, a signal is detected at 90 K. An identical spectrum is observed for a 90 K frozen DMF solution of $Cu(TFcP)\cdot 2DMF$ and this spectrum is shown in Figure 8. An analysis of this spectrum gives $g_\parallel = 2.185$, $g_\perp = 2.065$, and $A_\parallel(Cu) = 183$ G. Q-Band EPR spectra of $Cu(TFcP)\cdot 2DMF$ at both 300 and 100 K have been observed to have $g_\parallel$, $g_\perp$, and $A_\parallel(Cu)$ values essentially identical with those found in the 90 K X-band spectra.

The EPR spectral parameters for $Cu(TFcP)\cdot 2DMF$ are in good agreement with those obtained for other copper porphyrins.[57-60] Typically, values of $g_\parallel$ in the range of 2.170–2.190 and values of $g_\perp$ in the range of 2.040–2.080 are observed. The $A_\parallel(Cu)$ values are in the range of 184–206 G and $A_\perp(Cu)$ values are in the range of 34–42 G. The lower resolution of the perpendicular signal of $Cu(TFcP)\cdot 2DMF$ precludes a determination of the $A_\perp(Cu)$ value.

Oxidation Products of H_2TFcP and Cu(TFcP). Both H_2TFcP and Cu(TFcP) could potentially show several oxidation half-waves. Differential pulse polarography provides the best means to resolve nearby half-waves. The differential pulse polarogram of a CH_2Cl_2 solution of $H_2TFcP\cdot Me_2SO$ in Figure 9 shows a broad oxidation "wave" running from ca. 0.25 to 1.05 V vs. a SCE reference electrode. Ferrocene[61] shows a reversible wave at 0.41 V vs. SCE and free-base porphyrins and copper porphyrins have oxidation potentials greater than 0.8 V vs. SCE.[62]

The addition of either iodine dissolved in $CHCl_3$ or 2,3-dichloro-5,6-dicyano-1,4-benzoquinone (DDQ) dissolved in $CHCl_3$ to $CHCl_3$ solutions of H_2TFcP and Cu(TFcP) leads to the isolation of black compounds with the compositions $[H_2TFcP](X)_3$ and $[Cu(TFcP)](X)_2$, respectively, where X^- is either I_3^- or $DDQH^-$, the *diamagnetic* hydroquinone monoanion of DDQ. It is interesting that the free-base porphyrin is trioxidized, whereas the copper complex is only dioxidized. This difference probably reflects both differences in successive oxidation potentials as well as differences in solubilities of the various oxidation products. While H_2TFcP and Cu(TFcP) are both soluble in $CHCl_3$, Cu(TFcP) is considerably less soluble than H_2TFcP. The oxidation compounds are insoluble in chloroform, diethyl ether, ethanol, cyclohexane, acetone, acetonitrile, and benzene. Thus, although DDQ could potentially tetraoxidize both compounds, decreased solubilities preclude further oxidation beyond the $[H_2TFcP](X)_3$ and $[Cu(TFcP)](X)_2$ species.

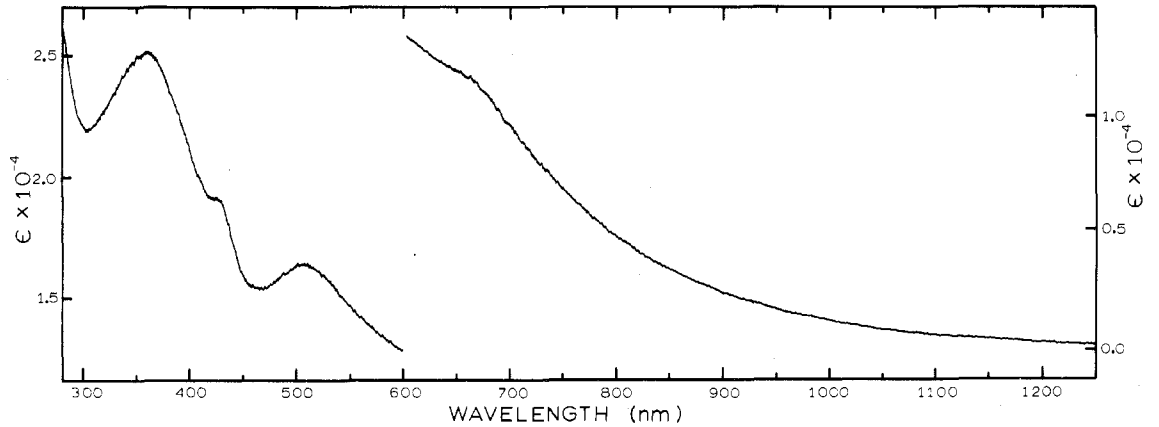

Figure 7. Room temperature electronic absorption spectrum of a $CHCl_3$ solution of $Cu(TFcP)\cdot DMF\cdot 2CHCl_3$. The molar extinction coefficient (ϵ) is given in units of M^{-1} cm^{-1}.

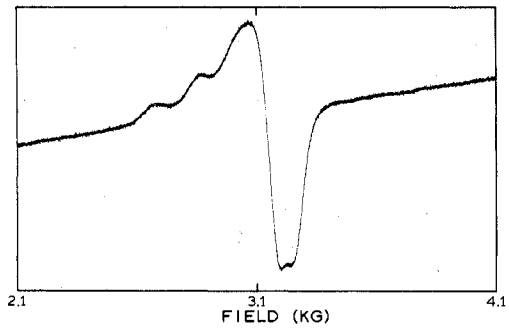

Figure 8. The 90 K, X-band EPR spectrum of a frozen DMF solution of Cu(TFcP)·2DMF.

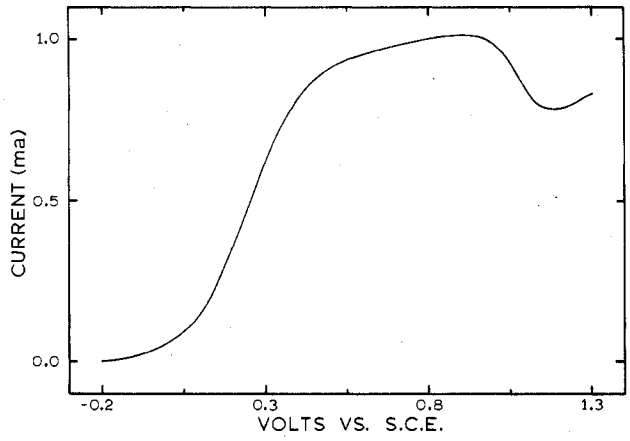

Figure 9. Differential-pulse polarogram of a CH_2Cl_2 solution of $H_2TFcP{\cdot}Me_2SO$. Voltages are referenced to a saturated calomel reference electrode.

The IR spectra of the oxidation compounds again show broad features that are very similar to those seen for the corresponding unoxidized compounds. Ferrocene bands at 500 and 1110 cm^{-1} are again seen. The ferricenium ion is known to have reduced infrared activity[63] and is not very visible in the spectra.

Variable-temperature magnetic susceptibility data were collected for three of the oxidized compounds. These measurements can help to further substantiate the number of oxidized ferrocenyl groups in each compound and determine whether there are any magnetic exchange interactions between the ferricenium moieties in a molecule. The variable-temperature (4.2–270 K) magnetic susceptibility data for $[H_2TFcP](I_3)_3$, $[H_2TFcP](DDQH)_3$, and $[Cu(TFcP)](I_3)_2$ are given in Tables I–III.[64] The effective magnetic moments per molecule at 270 K are 4.18 and 4.61 μ_B, respectively, for $[H_2TFcP](I_3)_3$ and $[H_2TFcP](DDQH)_3$. As the sample temperatures are decreased to 4.2 K, the effective magnetic moments gradually decrease to values of 3.13 and 3.33 μ_B, respectively. The decrease in μ_{eff} is somewhat more pronounced at the low temperature. A similar behavior is observed for $[Cu(TFcP)](I_3)_2$. The effective magnetic moment at 270 K is 4.85 μ_B and this decreases to 3.26 μ_B at 4.2 K.

The cations in $[H_2TFcP](I_3)_3$ and $[H_2TFcP](DDQH)_3$ possess three ferricenium moieties and each of these ferricenium centers is a $S = {}^1/_2$ system. The ferricenium ion has a $^2E_{2g}$ ground state which is split into two Kramers doublets by spin–orbit coupling and low-symmetry crystal fields. Simple ferricenium salts have effective magnetic moments at 300 K of 2.0–2.7 μ_B and these decrease with decreasing temperature down to values at or slightly below the spin-only value of 1.73 μ_B.[65] The μ_{eff} values *per ferricenium unit* in $[HTFcP](I_3)_3$ and $[H_2TFcP](DDQH)_3$ at 270 K are 2.42 and 2.76 μ_B, respectively. Both of these values tend to support the proposal that both of the compounds have three ferricenium moieties. Furthermore, the temperature curves for the μ_{eff} values (per ferricenium unit) are very characteristic of ferricenium systems. Thus there are no signs of magnetic exchange interactions between the ferricenium ions in either $[H_2TFcP](I_3)_3$ or $[H_2TFeP](DDQH)_3$.

The composition of $[Cu(TFcP)](I_3)_2$ suggests that there are *two* ferricenium moieties per cation. The Cu(II) ion is obviously also a $S = {}^1/_2$ system and as such the μ_{eff} values for this compound are very close to those for the other two oxidized compounds. Again, there is no indication of a magnetic exchange interaction.

The oxidized compounds are not soluble in any solvent suitable for electronic absorption spectra determination. However, spectra were obtained at 300 and 77 K for the oxidized compounds prepared as KBr pellets. No intervalence transfer (IT) bands were seen for any of these compounds in the visible or near-infrared regions. At 300 K, a resolved band at 290 nm and two partially resolved bands at 350 and 610 nm are observed for $[H_2TFcP](I_3)_3$. A resolved band at 365 nm and a partially resolved band at 270 nm are observed at 77 K. It is important to note that at the lower temperature the band at 610 nm apparently loses intensity. This is interesting in view of the fact that it is well-known that ferricenium ions exhibit a ligand-to-metal charge-transfer transition in the 600–650-nm region.[65,66] Usually this ferricenium band tends to increase in intensity at lower temperatures as a consequence of narrowing the bandwidth. Vibrational structure is also quite frequently observed.

For $[H_2TFcP](DDQH)_3$, a resolved band at 360 nm and a partially resolved band at ~250 nm are the only features seen at either 300 or 77 K. In the case of $[Cu(TFcP)](I_3)_2$, resolved bands at 262, 290, and 370 nm and partially resolved bands at 510 and 610 nm are observed at 300 K. Lowering the temperature of this copper compound to 77 K also leads to the disappearance of the band at 610 nm.

It is clear from the analytical and magnetic susceptibility data for the oxidized tetraferrocenylporphyrin compounds that these compounds are indeed formally mixed-valance compounds. The next point of interest is to characterize the thermal electron-transfer rates in these compounds. This can be effected by using the intrinsic time scales of different physical techniques.[12,13] Electron paramagnetic resonance is useful for such a study of mixed-valence ferrocene molecules. The compound $[Fe(cp)_2]I_3$ at 20 K in a glass shows a signal with $g_{\|} = 4.35$ and $g_{\perp} = 1.26$.[67] Biferrocene can be monooxidized to give biferricenium triiodide which as a pure solid at 12 K gives an EPR signal with $g_{\|} = 3.58$ and $g_{\perp} = 1.72$.[13] The biferricenium molecule is *localized* on the EPR time scale and the **g** tensor still shows the presence of considerable orbital angular momentum. On the other hand, the monooxidized bis(fulvalene)diiron cation is *delocalized* on the EPR time scale and, as an I_5^- salt, shows EPR signals even at room temperature with *g* values of 2.33 and 1.99.[13] As a solid, this same salt shows a very well-resolved signal at 12 K with *g* values of 2.36, 1.99, and 1.91. The **g** tensor for the EPR-delocalized system is *relatively* more isotropic. Finally, it is relevant to note that the EPR signal of the biferricenium cation depends on the anion with a $g_{\|}$ range of 3.34–4.38 and a $g_{\perp}$ range of 1.72–2.02.[13]

An X-band EPR signal is *not* observed at 300 K for a solid sample of $[H_2TFcP](I_3)_3$. At 90 K, however, signals are observed with *g* values of 4.35 and 2.60. The signals are very broad. The $g = 2.60$ signal has a line width (hwhm) of 1440 G. More highly resolved spectra are obtained at 90 K for $DMF/CHCl_3$ (1:1) and $Me_2SO/CHCl_3$ (1:1) frozen solutions of $[H_2TFcP](I_3)_3$. Both of these frozen-solution spectra have signals with *g* values of 4.30, 2.66, 1.96, and 1.78. The 90 K $DMF/CHCl_3$ solution spectrum is shown in Figure 10. Very

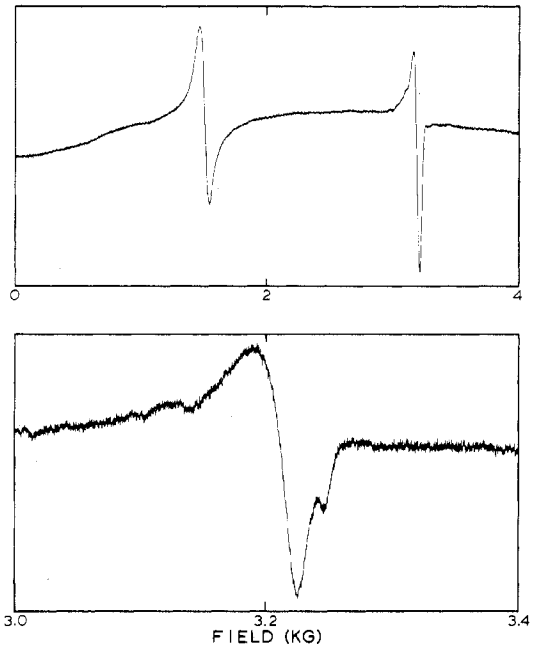

Figure 10. The 90 K, X-band EPR spectrum of a frozen DMF/$CHCl_3$ (1:1) solution of $[H_2TFcP](I_3)_3$.

Table IV. Electron Paramagnetic Resonance Data

Compd	Sample condition	X band 300 K	X band 90 K	X band 8 K	Q band 300 K	Q band 100 K
$[TFcP](I_3)_3$	Solid	NS[a]	4.35 2.60	NS[a]	2.00	2.00
	Glass[e]		4.30[b] 2.66 1.96 1.78			
[TFcP]-$(DDQH)_3$	Solid	NS[a]	4.32[b] 2.02	4.30[b] 2.02	4.46[d] 2.00	4.46[d] 2.00
	Glass[f]		4.28[b] 4.16 2.33 2.02[g]			
[Cu(TFcP)]-$(I_3)_2$	Solid	NS[a]	2.19[h] 2.02	2.07[b,c]	2.14[i] 2.07	2.14[i] 2.07
	Glass[e]			3.24[d] 2.17[h] 2.04 2.00		

[a] NS = no signal. [b] Unresolved shoulder on low field side of signal. [c] Unresolved shoulder on high field side of signal. [d] Weak. [e] DMF/$CHCl_3$ (1:1). [f] $Me_2SO/CHCl_3$ (1:1). [g] Two signals: one broad and one very sharp. [h] $A_{\parallel}(Cu) = 195$ G. [i] Unresolved $A_{\parallel}(Cu)$.

broad $g = 2.00$ Q-band signals are observed for a solid sample of $[H_2TFcP](I_3)_3$ at 300 and 100 K which have line widths (hwhm) of 2550 G. Perhaps the most unusual and interesting EPR observation on $[H_2TFcP](I_3)_3$ is that *no* X-band EPR signal is observed for the pure solid at 8 K. The broad line widths for the ferricenium-like solid at ~90 K would be expected to narrow markedly when the sample is cooled to liquid-helium temperatures rather than disappear.

Similar overall EPR characteristics were found for $[H_2TFcP](DDQH)_3$. Table IV summarizes the EPR signals for the oxidized H_2TFcP compounds. Only two basic differences were observed for the $DDQH^-$ salt as compared to the I_3^- salt. First, there is a very narrow $g = 2.02$ signal for the $DDQH^-$ salt. This is most likely associated with some small amount of $DDQ^-\cdot$ semiquinone present in the solid. As demonstrated previously for mixed-valence bifferocene compounds with quinone-type counterions,[61] the major counterion is the diamagnetic hydroquinone anion, $DDQH^-$, and $DDQ^-\cdot$ is only a very small impurity anion. The second difference is that, unlike the I_3^- salt, the $DDQH^-$ salt does show an X-band spectrum for a pure solid at 8 K; however, the signal is weak.

Table V. Iron-57 Mössbauer Fitting Parameters[a]

Compd	Temp, K	δ,[b] mm/s	ΔE_Q, mm/s	Rel area
$[H_2TFcP](I_3)_3$	295	0.376 (40)	2.200 (40)	0.25
		0.292 (17)	0.766 (17)	0.75
	90	0.431 (4)	2.185 (4)	0.50
		0.385 (7)	0.686 (7)	0.50
	4.2	0.443 (3)	2.192 (3)	0.67
		0.445 (2)	0.496 (2)	0.33
$[H_2TFcP](DDQH)_3$	295	0.344 (19)	2.214 (19)	0.50
		0.264 (65)	0.811 (65)	0.50
	100	0.410 (3)	2.201 (3)	0.63
		0.367 (14)	0.776 (14)	0.37
	4.2	0.448 (2)	2.262 (2)	0.77
		0.425 (21)	0.743 (21)	0.23
$[Cu(TFcP)](I_3)_2$	295	0.350 (13)	2.249 (13)	0.50
		0.293 (47)	0.860 (47)	0.50
	90	0.430 (4)	2.236 (4)	0.50
		0.387 (88)	0.265 (88)	0.50
	4.2	0.442 (2)	2.242 (2)	0.67
		0.414 (25)	0.492 (25)	0.33
H_2TFcP	100	0.415 (6)	2.270 (6)	1.0

[a] Error in last significant figure given in parentheses. [b] Relative to iron metal.

The EPR characteristics of $[Cu(TFcP)](I_3)_2$ are also summarized in Table IV. Copper hyperfine is seen on the 8 K DMF/$CHCl_3$ (1:1) glass spectrum where $A_{\parallel}(Cu)$ is 195 G, which is ca. 10 G larger than that observed for unoxidized Cu(TFcP). The 8 K X-band spectrum for the pure solid shows only a relatively weak signal at $g = 2.07$.

In summary, the EPR spectra of the oxidized tetraferrocenylporphyrin compounds point to EPR-localized ferricenium centers. Thus, the thermal electron-transfer rates between ferrocene and ferricenium centers must be less than ca. 10^9 s^{-1}. One other point stands out. The ferricenium centers in these compounds tend to show weak or nonexistent EPR signals for the solids at 8 K. As we turn to the ^{57}Fe Mössbauer results, the comment about thermal electron-transfer rates will be substantiated and insight will be provided about the peculiar low-temperature EPR characteristics.

Iron-57 Mössbauer spectroscopy is particularly useful for mixed-valence iron metallocenes.[13] A mixed-valence compound with a thermal electron-transfer rate less than ca. 10^7 s^{-1} will show two doublets, one for each of the two different iron sites (i.e., ferrocene and ferricenium) and the molecule is said to be localized on the Mössbauer time scale. A mixed-valence compound with a thermal electron-transfer rate greater than ca. 10^7 s^{-1} will show only one doublet with an average isomer shift and an average quadrupole splitting. In the case of the oxidized tetraferrocenylporphyrin compounds ^{57}Fe Mössbauer spectra are also useful to tell the relative number of ferrocene and ferricenium centers. This information comes from the integrated areas (via least-squares fitting) of the two doublets.

Ferrocene and ferricenium quadrupole-split doublets are observed in the Mössbauer spectrum for each of the oxidized compounds. Each spectrum has been least-squares fit to Lorentzian lines. The two components of each doublet were constrained to have equal areas. Mössbauer data were collected for each of the oxidized compounds at three temperatures and the resultant fitting parameters are given in Table V.

The most interesting observation in this study is that the Mössbauer spectra for the oxidized compounds are tem-

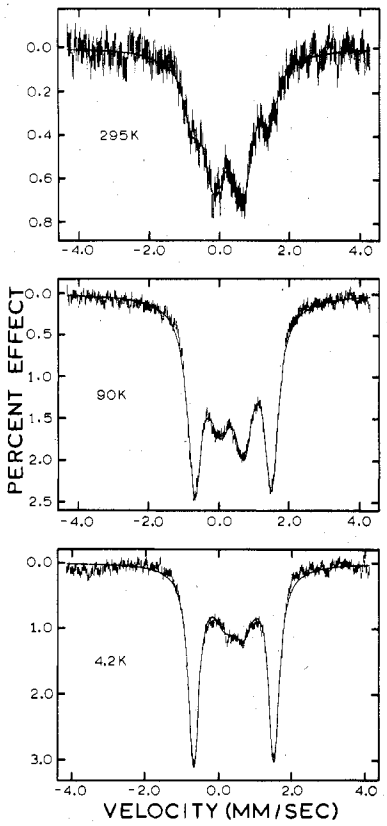

Figure 11. The ^{57}Fe Mössbauer spectra of $[H_2TFcP](I_3)_3$ at 295, 90, and 4.2 K. The velocity scale is referenced to iron metal.

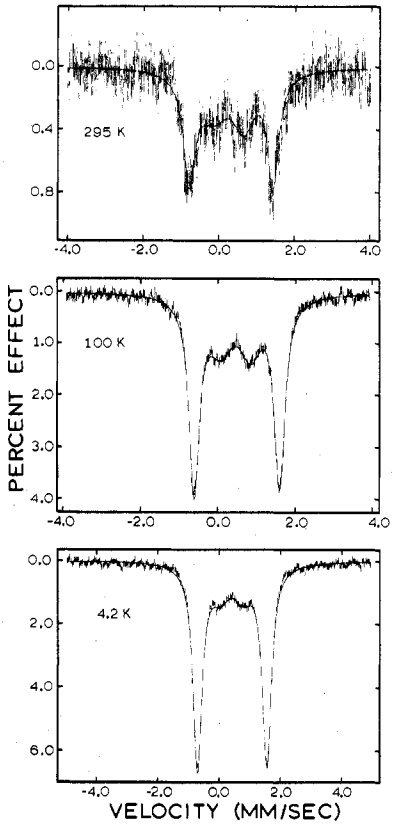

Figure 12. The ^{57}Fe Mössbauer spectra of $[H_2TFcP](DDQH)_3$ at 295, 100, and 4.2 K. The velocity scale is referenced to iron metal.

perature dependent. The spectra of $[H_2TFcP](I_3)_3$ at 295, 90, and 4.2 K are shown in Figure 11. The relative areas of the two types of iron centers are obviously strongly temperature dependent. The two outermost features comprise the ferrocene doublet. The relative area of the ferrocene doublet increases while the relative area of the ferricenium doublet decreases as the temperature of the sample is lowered. Quantitatively, the ferrocene-to-ferricenium area ratios at 295, 90, and 4.2 K are 1:3, 1:1, and 2:1, respectively. The 1:3 ferrocene to ferricenium relative area ratio at 295 K is as expected for $[H_2TFcP](I_3)_3$ if three of the ferrocene groups are oxidized.

Least-squares fitting of the $[H_2TFcP](I_3)_3$ spectra also shows that, taking into account the poor statistics associated with the 295 K spectrum, the isomer shifts relative to iron metal of 0.38–0.44 mm/s and quadrupole splittings of 2.19–2.20 mm/s *for the ferrocene centers* are relatively temperature independent. However, *for the ferricenium centers* the isomer shifts increase from 0.29 mm/s at 295 K to 0.45 mm/s at 4.2 K, and the quadrupole splittings decrease from 0.77 mm/s at 295 K to 0.50 mm/s at 4.2 K. Although not explicitly pointed out previously, the Mössbauer parameters obtained for other formally mixed-valence biferrocene systems also exhibit similar temperature-dependent ferricenium isomer shifts and quadrupole splittings.[13]

Figure 12 illustrates the Mössbauer data obtained for $[H_2TFcP](DDQH)_3$. The ferrocene-to-ferrocenium area ratio is also temperature dependent for this compound; however, the ratios are different. At 295, 100, and 4.2 K, the quantitative area ratios for $[H_2TFcP](DDQH)_3$ are 1:1, 1.7:1, and 3.3:1, respectively. As with the other compound, the isomer shifts and quadrupole splittings for the ferrocene centers are relatively temperature independent, while the isomer shifts increase and the quadrupole splittings decrease for the ferricenium centers as the temperature decreases.

The same type of temperature dependences of isomer shifts and quadrupole splittings for the ferrocene and ferricenium

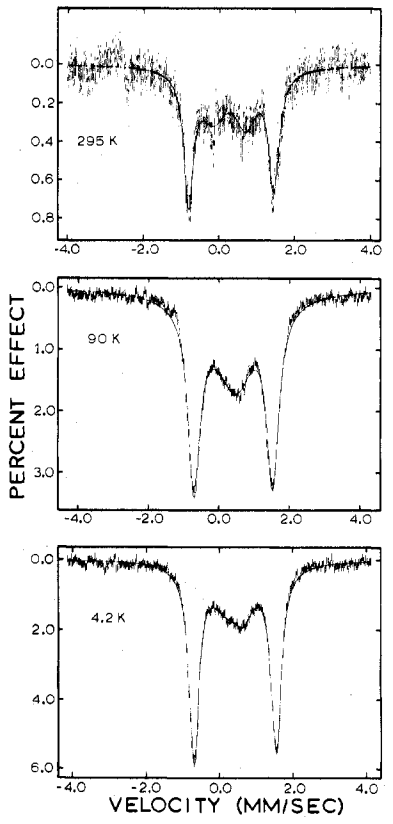

Figure 13. The ^{57}Fe Mössbauer spectra of $[Cu(TFcP)](I_3)_2$ at 295, 90, and 4.2 K. The velocity scale is referenced to iron metal.

centers are observed for $[Cu(TFcP)](I_3)_2$. However, the ferrocene-to-ferricenium area ratios are, again, different at 295, 90, and 4.2 K. The spectra are shown in Figure 13. In

this case, the quantitative area ratios are 1:1, 1:1, and 2:1, respectively. In all three of these oxidized compounds the Mössbauer parameters and their temperature dependences are similar to those reported for mixed-valence biferrocenes.[13] The temperature dependence of ferrocene-to-ferricenium ratio has only been noted in one other system, the oxidized [1.1]-ferrocenophanes.[14] The disappearance of the 610-nm band in the low-temperature electronic spectra and the relatively weak ferricenium EPR signal at 8 K are also apparently reflections of the decreasing ferricenium content at low temperatures.

The decrease in the numbers of ferricenium centers and concurrent increase in the number of ferrocene centers with decreasing temperature are, indeed, quite dramatic. Different temperature-dependent ferrocene and ferricenium recoilless fractions are not a possible explanation for this effect. In a given spectrum, the integrated area of the energy distribution of a Mössbauer absorption is proportional to the probability, f, for recoilless absorption. This probability is related to the energy of the absorbed γ photon, E_γ, and the mean-square amplitude of vibration, $\langle x^2 \rangle$, of the absorbing atom in the direction of propagation of the γ photon. The f relation is given as[68]

$$f \propto \exp[-(E_\gamma/\hbar c)^2 \langle x^2 \rangle]$$

The only temperature-dependent term in this expression for f is $\langle x^2 \rangle$. There is very little amplitude of vibration for any atom at 4.2 K and as such the recoilless fractions for the ferrocene and ferricenium iron atoms would be equal. The 2:1 area ratio for $[H_2TFcP](I_3)_3$ indicates that there are twice as many ferrocenes as ferricenium ions in this molecule. Assuming that the number of ferrocene-to-ferricenium ions remains 2:1 at 295 K, the observed change of area ratio to 1:3 indicates that $\langle x^2 \rangle$ for iron ions of the ferrocene centers is 5 times greater than for the iron ions of the ferricenium centers and is on the order of 0.2 Å. Clearly, this in unrealistic. At best, only very small differences in the temperature dependences of $\langle x^2 \rangle$ for an iron ion of a ferrocene and a ferricenium ion are expected, particularly when both ions are part of the same molecule. Thus, it may be safely concluded that the temperature-dependent changes of the relative areas of the ferrocene and the ferricenium centers do indicate a change in the number of ferrocene and ferricenium centers and not simply a difference in recoilless fraction temperature dependences.

Since the magnetic susceptibility data do not indicate a change of spin state (i.e., three unpaired electrons) with decreasing temperature for any of the three oxidized salts, the conversion of ferricenium centers into ferrocene centers in a given molecule is proposed to occur by unpaired electron density migration from the ferricenium centers to the porphyrin ring at low temperatures. Thus, at the low temperatures there is a mixture of some amount of ferricenium centers each with an unpaired electron and porphyrin π-cation radicals. Such π-cation radicals are known of course. A previous EPR investigation together with molecular orbital calculations indicates that high-spin density may be located at the C_m carbon atoms of some porphyrin cation radicals.[69] Thus, localized rather than delocalized radicals may be present at low temperatures for the $[H_2TFCP](X)_3$ and $[Cu(TFcP)](I_3)_2$ compounds. The EPR signals that have g values of 1.96, 2.02, and 2.00, respectively, for frozen solutions of $[H_2TFcP](I_3)_3$, $[H_2TFcP](DDQH)_3$, and $[Cu(TFcP)](I_3)_2$ may possibly be attributable to these porphyrin cation radicals.

The proposed temperature-dependent migration of unpaired electron density may well be a consequence of small temperature-dependent structural changes. In the above discussion of the anomalous electronic absorption spectrum of H_2TFcP, it was argued that the small dihedral angle between the planes of the substituted cyclopentadienyl ring of the ferrocenyl group and the porphyrin ring allows the π systems of the two rings to strongly interact. This interaction, which can be reflected in the magnitude of overlap integrals between the appropriate orbitals, is expected to increase as the dihedral angle decreases from 90 to 0°. For these oxidized compounds, the presence of counterions in the crystal lattice would be expected to change the static equilibrium dihedral angle as compared to that of the unoxidized compounds. In addition, small temperature-dependent changes in crystal lattice packing arrangements induced by the counterions could very easily cause temperature-dependent changes of the dihedral angle. The change in dihedral angle does not have to be very large (5–10°) to cause significant changes. The consequences are that, as the dihedral angle approaches or recedes from 0°, the interaction between the π systems of the two rings will increase or decrease, and unpaired electron density migration to the porphyrin ring from the ferricenium centers will be facilitated or hindered accordingly. Different counterions would be expected to cause different temperature dependences. This is supported quite nicely by the different temperature-dependent area ratios observed in the Mössbauer spectra of $[H_2TFcP](I_3)_3$ and $[H_2TFcP](DDQH)_3$.

It appears that the unpaired electron density migration is *not* peculiar just to tetraferrocenylporphyrin. In a forthcoming paper,[70] we will detail the mixed-valence chemistry of oxidized compounds resulting from

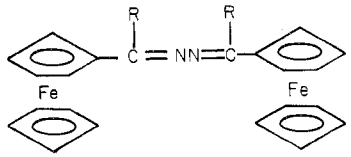

R = H, CH_3

Temperature-dependent ferrocene-to-ferricenium ratios are found in the Mössbauer spectra of these compounds.

Concluding Remarks

Although many of the chemical and physical properties of H_2TFcP and Cu(TFcP) were found to be similar to other meso-substituted porphyrins and metalloporphyrins, there are differences which seem to reflect the bulky nature of the ferrocenyl groups and the possible interaction of the ferrocenyl and porphyrin π systems. The oxidation products, $[H_2TFcP](X)_3$ and $[Cu(TFcP)](X)_2$, provided a means of investigating magnetic exchange interactions propagated by a fragment of the porphyrin unit. No evidence of such an interaction was found. This means that there is no exchange interaction between ferricenium centers on nearby methine positions or between the Cu(II) ion and a ferricenium center. As a consequence, the rate of *electron exchange* between these pairs of paramagnetic centers is small. Based on the temperature-dependent Mössbauer data, it was deduced that small orientational changes of the ferrocenyl groups relative to the plane of the porphyrin were found to result in unpaired electron density migration from the ferricenium centers to the porphyrin ring. It would seem that the porphyrin π-cationic radical nature that is found at low temperatures would be required to be somewhat localized; otherwise the mixed-valence ferrocene–ferricenium centers would have greater thermal electron-transfer rates. The significance of these results as they relate to various studies on cytochrome *c* reflects the information that they give on the viability of electron dynamics between different parts of a porphyrin. E.g., can an electron transfer from the exposed methine position of cytochrome *c* to the iron ion? Further studies of this type are needed, and it is not suggested that a ferricenium center is the best probe

of electron dynamics at the methine carbon of a porphyrin.

Acknowledgment. We thank Professor P. G. Debrunner and Mr. C. R. Hill for assistance with the ^{57}Fe Mössbauer work. We are grateful for partial funding of this research by National Institutes of Health Grant HL 13652.

Registry No. $H_2TFcP \cdot Me_2SO$, 64130-67-2; $H_2TFcP \cdot 2CHCl_3$, 64130-66-1; Cu(TFcP)·2DMF, 64130-64-9; Cu(TFcP)·DMF·$2CHCl_3$, 64130-63-8; $[H_2TFcP](I_3)_3$, 64130-61-6; $[H_2TFcP](DDQH)_3$, 64130-60-5; $[Cu(TFcP)](I_3)_2$, 64130-58-1; formylferrocene, 12093-10-6; pyrrole, 109-97-7.

Supplementary Material Available: Tables I–III, listings of magnetic susceptibility data (3 pages). Ordering information is given on any current masthead page.

References and Notes

(1) Camille and Henry Dreyfuss Teacher–Scholar Fellow, 1972–1977; A. P. Sloan Foundation Fellow, 1976–1978.
(2) K. M. Smith, Ed., "Porphyrins and Metalloporphyrins", Elsevier, New York, N.Y., 1975.
(3) G. R. Moore, and R. J. P. Williams, *Coord. Chem. Rev.*, **18**, 125 (1976).
(4) R. W. Holwerda, J. Rawlings, and H. B. Gray, *Annu. Rev. Biophys. Bioeng.*, **5**, 363 (1976).
(5) H. A. Harbury and R. H. L. Marks in "Inorganic Biochemistry", Vol. 2, G. L. Eichhorn, Ed., Elsevier, New York, N.Y., 1973.
(6) R. E. Dickerson, T. Takano, D. Eisenberg, O. B. Kallai, L. Samson, A. Cooper, and E. Margoliash, *J. Biol. Chem.*, **246**, 1511 (1971).
(7) T. Takano, O. B. Kallai, R. Swanson, and R. E. Dickerson, *J. Biol. Chem.*, **248**, 5234 (1974).
(8) R. E. Dickerson, *Ann. N.Y. Acad. Sci.*, **227**, 599 (1974).
(9) F. R. Salemme, J. Kraut, and M. D. Kamen, *J. Biol. Chem.*, **248**, 7701 (1973).
(10) C. J. Grimes, D. Piszkiewicz, and E. B. Fleischer, *Proc. Natl. Acad. Sci. U.S.A.*, **71**, 1408 (1974).
(11) M. A. Ratner and M. J. Ondrechen, *Mol. Phys.*, **32**, 1233 (1976).
(12) R. G. Wollmann and D. N. Hendrickson, *Inorg. Chem.*, **16**, 723 (1977).
(13) W. H. Morrison, Jr., and D. N. Hendrickson, *Inorg. Chem.*, **14**, 2331 (1975).
(14) W. H. Morrison, Jr., and D. N. Hendrickson, *Chem. Phys. Lett.*, **22**, 119 (1973); W. H. Morrison, Jr., and D. N. Hendrickson, *J. Chem. Phys.*, **59**, 380 (1973).
(15) R. F. Kirchner, G. H. Loew, and U. T. Mueller-Westerhoff, *Inorg. Chem.*, **15**, 2665 (1976).
(16) A. D. Adler, F. R. Longo, J. O. Finarelli, J. Goldmacher, J. Assour, and L. Korsakoff, *J. Org. Chem.*, **32**, 476 (1967).
(17) A. D. Adler, F. R. Longo, F. Kampas, and J. Kim, *J. Inorg. Nucl. Chem.*, **32**, 2443 (1970).
(18) G. R. Hall and D. N. Hendrickson, *Inorg. Chem.*, **15**, 607 (1976).
(19) E. Munck, P. G. Debrunner, J. C. M. Tsibris, and I. C. Gunsalus, *Biochemistry*, **11**, 855 (1972).
(20) C. R. Hill and P. G. Debrunner, unpublished results.
(21) B. L. Chrisman and T. A. Tumolillo, *Comput. Phys. Commun.*, **2**, 322 (1971).
(22) G. H. Barnett, M. F. Hudson, and K. M. Smith, *Tetrahedron Lett.*, 2887 (1973).
(23) K. Rousseau and D. Dolphin, *Tetrahedron Lett.*, 4251 (1974).
(24) J. B. Kim, J. J. Leonard, and F. R. Longo, *J. Am. Chem. Soc.*, **94**, 3986 (1972).
(25) A. D. Adler, L. Sklar, F. R. Longo, J. D. Finarelli, and M. G. Finarelli, *J. Heterocycl. Chem.*, **5**, 669 (1968).
(26) A. H. Corwin and E. C. Coolidge, *J. Am. Chem. Soc.*, **74**, 5196 (1952).
(27) D. Dolphin, *J. Heterocycl. Chem.*, **7**, 275 (1970).
(28) S. J. Silvers and A. Tulinsky, *J. Am. Chem. Soc.*, **89**, 3331 (1967).
(29) B. M. L. Chen and A. Tulinsky, *J. Am. Chem. Soc.*, **94**, 4144 (1972).
(30) J. D. Dunitz, L. E. Orgel, and A. Rich, *Acta Crystallogr.*, **9**, 373 (1956).
(31) Z. Kaluski, *Bull. Acad. Pol. Sci., Ser. Sci. Chim.*, **12**, 873 (1964).
(32) A. Wolberg, *J. Mol. Struct.*, **21**, 61 (1974).
(33) L. K. Gottwald and E. F. Ullman, *Tetrahedron Lett.*, 3071 (1969).
(34) F. A. Walker and G. L. Avery, *Tetrahedron Lett.*, 4949 (1971).
(35) J. P. Collman, R. R. Gagne, C. A. Reed, T. R. Halbert, G. Lang, and W. T. Robinson, *J. Am. Chem. Soc.*, **97**, 1427 (1975).
(36) K. N. Solov'ev, V. A. Mashenkov, A. T. Gradyushko, A. E. Turkova, and V. P. Lezina, *J. Appl. Spectrosc. (Engl. Transl.)*, **13**, 1106 (1970).
(37) C. B. Storm, Y. Teklu, and E. A. Sokolski, *Ann. N.Y. Acad. Sci.*, **206**, 631 (1973).
(38) N. Kamezawa, *J. Magn. Resonan.*, **11**, 88 (1973).
(39) R. J. Abraham, G. E. Hawkes, M. F. Hudson, and K. M. Smith, *J. Chem. Soc., Perkin Trans. 2*, 204 (1975).
(40) S. S. Eaton and G. R. Eaton, *Inorg. Chem.*, **15**, 134 (1976).
(41) A. N. Nesmeyanov, G. B. Shul'pin, M. I. Rybinskaya, and P. V. Petrovskii, *Dokl. Akad. Nauk SSSR*, **215**, 599 (1974).
(42) G. K. Wertheim and R. H. Herber, *J. Chem. Phys.*, **38**, 2106 (1963).
(43) T. C. Gibb, *J. Chem. Soc., Dalton Trans.*, 1237 (1976).
(44) J. O. Alben, S. S. Choi, A. D. Adler, and W. S. Caughey, *Ann. N.Y. Acad. Sci.*, **206** 278 (1973).
(45) D. Hartley and M. J. Ware, *J. Chem. Soc. A*, 138 (1969).
(46) I. J. Hyams, *Spectrochim. Acta, Part A*, **29a**, 839 (1973).
(47) A. Treibs and N. Häberle, *Justus Liebigs Ann. Chem.*, **718**, 183 (1968).
(48) P. W. Codding and A. Tulinsky, *J. Am. Chem. Soc.*, **94**, 4151 (1972).
(49) J. W. Lauher and J. A. Ibers, *J. Am. Chem. Soc.*, **95**, 5148 (1973).
(50) R. G. Little and J. A. Ibers, *J. Am. Chem. Soc.*, **97**, 5363 (1975).
(51) L. J. Boucher, *Coord. Chem. Rev.*, **7**, 289 (1972).
(52) J. A. Shelnutt, D. C. O'Shea, N.-T. Yu, L. D. Cheung, and R. H. Felton, *J. Chem. Phys.*, **64**, 1156 (1976).
(53) N. J. Gogan and Z. U. Siddiqui, *Can. J. Chem.*, **50**, 720 (1972).
(54) L. Edwards and M. Gouterman, *J. Mol. Spectrosc.*, **33**, 292 (1970).
(55) A. M. Schaffer and M. Gouterman, *Theor. Chim. Acta*, **25**, 62 (1972).
(56) A. Henriksson and M. Sundbom, *Theor. Chim. Acta*, **27**, 213 (1972).
(57) E. M. Roberts and W. S. Koski, *J. Am. Chem. Soc.*, **82**, 3006 (1960).
(58) J. M. Assour, *J. Chem. Phys.*, **43**, 2477 (1965).
(59) P. T. Manoharan and M. T. Rogers in "Electron Spin Resonance of Metal Complexes", T. F. Yen, Ed., Plenum Press, New York, N.Y., 1969.
(60) J. Subramanian, J.-H, Fuhrhop, A. Salek, and A. Gossauer, *J. Magn. Reson.*, **15**, 19 (1974).
(61) W. H. Morrison, Jr., S. Krogsrud, and D. N. Hendrickson, *Inorg. Chem.*, **12**, 1998 (1973).
(62) J.-H. Fuhrhop, *Struct. Bonding (Berlin)*, **18**, 1 (1974).
(63) D. M. Duggan and D. N. Hendrickson, *Inorg. Chem.*, **14**, 955 (1975).
(64) Supplementary material.
(65) D. N. Hendrickson, Y. S. Sohn, and H. B. Gray, *Inorg. Chem.*, **10**, 1559 (1971).
(66) D. N. Hendrickson, Y. S. Sohn, D. M. Duggan, and H. B. Gray, *J. Chem. Phys.*, **58**, 4666 (1973).
(67) S. E. Anderson and R. Rai, *Chem. Phys.*, **2**, 216 (1973); R. Prins and A. Kortbeek, *J. Organomet. Chem.*, **33**, C33 (1971).
(68) N. N. Greenwood and T. C. Gibb, "Mössbauer Spectroscopy", Chapman and Hall, London, 1971.
(69) J. Fajer, D. C. Borg, A. Forman, R. H. Felton, L. Vegh, and D. Dolphin, *Ann. N.Y. Acad. Sci.*, **206** 349 (1973).
(70) R. G. Wollmann and D. N. Hendrickson, manuscript in preparation.